Analyst

ROYAL SOCIETY OF CHEMISTRY

COMMUNICATION

View Article Online
View Journal

Published on 20 February 2025. Downloaded by Shanghai Normal University on 2/26/2025 3:10:55 AM.

Check for updates

Cite this: DOI: 10.1039/d5an00031a

Received 9th January 2025,
Accepted 19th February 2025

DOI: 10.1039/d5an00031a

rsc.li/analyst

A novel biosensor for highly sensitive DNA damage detection using TdT and CRISPR-Cas12a†

Juan Wang,‡[a] Fan Zhang,‡[b] Ziyang Liu,[a] Yue Zhou,[a] Liguo Pei*[c] and Bei Yan *[a,d]

This study presents a highly sensitive fluorescence biosensor integrating TdT enzyme and CRISPR-Cas12a for precise detection of sperm DNA damage, achieving a detection limit of 0.99 pM and a linear range of 0.001–0.2 nM. Its exceptional sensitivity, simplicity, and versatility make it a transformative tool for reproductive medicine and clinical diagnostics.

DNA damage is prevalent in mammalian reproductive cells. Maintaining the integrity of sperm DNA is crucial for the stable inheritance of paternal genetic material.[1–3] Sperm DNA damage impairs reproductive capacity and poses substantial risks to the genetic stability and health of offspring.[4] The most common types of sperm DNA damage are single-strand breaks (SSBs) and double-strand breaks (DSBs), which are predominantly induced by oxidative stress. Oxidative radicals (*e.g.*, hydroxyl radicals) and external factors, including ionizing radiation, directly or indirectly cause DNA fragmentation, thereby impairing sperm function and reducing fertilization capacity.[5–8]

Advances in assisted reproductive technologies (ART), particularly intracytoplasmic sperm injection (ICSI), enable sperm with DNA damage to bypass natural selection and directly fertilize oocytes. While oocytes and zygotes can repair DNA damage to a certain degree, excessive damage exceeding their repair threshold may lead to defective DNA transmission, heightening the risk of hereditary diseases.[9–12] The accurate detection and evaluation of sperm DNA damage have become pressing priorities in modern reproductive medicine. Existing methods for detecting sperm DNA fragmentation (SDF) primarily include the sperm chromatin dispersion test (SCD),[13,14] the sperm chromatin structure assay (SCSA),[15–17] terminal deoxynucleotidyl transferase dUTP nick end labeling (TUNEL),[18–20] and the comet assay. Although these methods are widely applied in both clinical and research settings, they are limited by issues such as low sensitivity, operational complexity, high cost, and subjective result interpretation.[21] For example, the SCD method is fast and simple but susceptible to operator subjectivity. The SCSA method is highly accurate but necessitates expensive flow cytometry equipment, which limits its widespread use. The TUNEL method is time-consuming and prone to interference, whereas the comet assay, though intuitive, depends on subjective interpretation. Furthermore, existing evaluation metrics, such as the sperm DNA fragmentation index (DFI), cannot accurately quantify the extent of sperm DNA damage, underscoring the demand for more precise and efficient detection methods. A prior study introduced a TdT-based approach integrated with a strand displacement probe, aiming to enhance the precision of sperm DNA damage assessment.[22] However, its sensitivity remained suboptimal, with a detection limit of 0.01 nM.[22]

To address these limitations, this study develops an innovative fluorescence detection system for sperm DNA breakpoints, combining enzyme technology, the CRISPR-Cas12a system, and a PCR-based platform. The CRISPR-Cas12a RNA-guided complex holds great promise for nucleic acid detection.[23]

As shown in Fig. 1, TdT recognizes the 3′-OH ends of sperm DNA breakpoints and extends them with polyadenosine (poly-A) sequences. Guided by crRNA, the CRISPR-Cas12a system specifically recognizes poly-A sequences, activating its *trans*-cleavage activity to cleave a single-stranded fluorescence probe. This cleavage separates FAM from BHQ-1, producing a strong fluorescent signal.[24] The fluorescence intensity rate is positively correlated with the number of poly-A sequences and, consequently, the number of sperm DNA breakpoints. This novel system enabled precise quantification of DNA break-

[a]*Key Laboratory of Fertility Preservation and Maintenance of Ministry of Education, Ningxia Medical University, Institute of Medical Sciences, General Hospital of Ningxia Medical University, Yinchuan, 750004, China.*
E-mail: d202081630@alumni.hust.edu.cn
[b]*Reproductive Medical Center, Yinchuan women and children healthcare hospital, Yinchuan, 750001, China*
[c]*Reproductive Medical Center, General Hospital of Ningxia Medical University, Yinchuan, 750004, China. E-mail: 18295182917@163.com*
[d]*Tongji Medical College, Huazhong University of Science and Technology, Wuhan, 430030, China*

†Electronic supplementary information (ESI) available: Details of experimental procedures and additional figures. See DOI: https://doi.org/10.1039/d5an00031a

‡These authors contributed equally.

Published on 20 February 2025. Downloaded by Shanghai Normal University on 2/26/2025 3:10:55 AM.

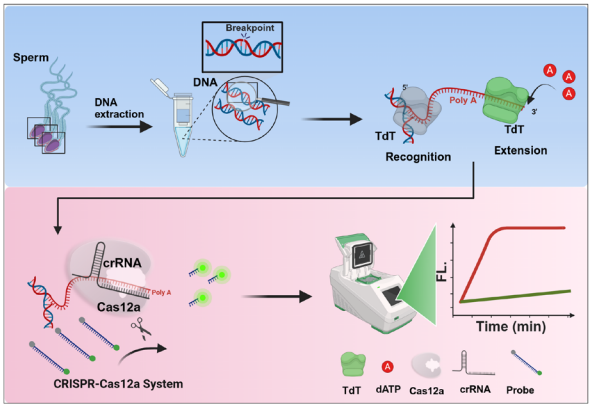


Fig. 1 Schematic illustration of the working principle of the biosensor.

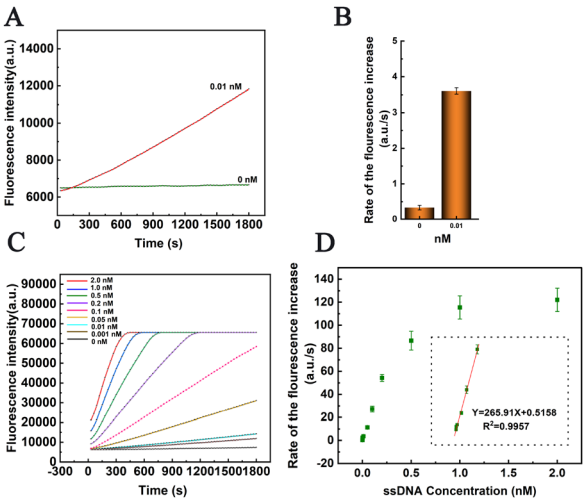


Fig. 2 (A) Fluorescence curves of the biosensor in the presence and absence of the DNA substrate. (B) Fluorescence signal increase rates of the biosensor under conditions with and without the DNA substrate. (C) Fluorescence intensity of the biosensor at different ssDNA concentrations: 0, 0.001 nM, 0.01 nM, 0.05 nM, 0.1 nM, 0.2 nM, 0.5 nM, 1 nM, and 2 nM. (D) Standard curve illustrating the relationship between the fluorescence signal increase rate and ssDNA concentration.

points, providing a more accurate assessment of sperm DNA fragmentation levels. Additionally, we explored the application of this detection system for assessing DNA damage in other reproductive cells, including spermatogonial stem cells. This technology not only addresses the limitations of traditional methods but also serves as a valuable tool for investigating DNA damage and repair mechanisms.

Verification of the biosensor's working principle

To validate the functionality of the novel biosensor, synthetic single-stranded DNA (ssDNA) was used as the substrate. ssDNA samples at varying concentrations (0, 0.001 nM, 0.01 nM, 0.05 nM, 0.1 nM, 0.2 nM, 0.5 nM, 1 nM, and 2 nM) were prepared and incubated with TdT at 37 °C for 30 minutes. After thermal inactivation of TdT, a fluorescence reporter system containing Cas12a was introduced. The crRNA recognized the poly-A sequence extended by TdT at DNA break sites, activating the *trans*-cleavage activity of the Cas12a system. This activity cleaved the single-stranded fluorescent probe, separating FAM from BHQ-1 and producing a strong fluorescence signal.[25]

As shown in Fig. 2A, the blank control group (no added DNA substrate) exhibited negligible fluorescence, while the addition of 0.01 nM substrate DNA resulted in a significant fluorescence increase. The rate of fluorescence signal increase was subsequently calculated (Fig. 2B). Key parameters of the fluorescence reporter system were systematically optimized to enhance detection performance. These parameters included Cas12a and crRNA concentrations, buffer composition, Mg^{2+} levels, probe length, and probe concentration (ESI, Fig. S1†).

Under optimized conditions (Cas12a: 100 nM; crRNA: 200 nM; NEBuffer 4; 15-nt probe; 500 nM probe), fluorescence curves were generated for varying substrate DNA concentrations (Fig. 2C). A linear equation was then fitted to describe the relationship between fluorescence signal increase rate and substrate DNA concentration. The linear detection range was identified as 0.001–0.2 nM (Fig. 2D), with a limit of detection (LOD) of 0.99 pM, calculated using the formula $3\sigma/k$.

Compared to previously reported sensors for detecting DNA breakpoints,[21,22] this system achieves a significant improvement in detection limit, demonstrating higher sensitivity and greater application potential.

The number of DNA break sites can be calculated by substituting the fluorescence signal increase rate of the test sample into the linear equation. Detailed calculation formulas are provided in the ESI (section 1.43†).

To assess the feasibility of the sensor for detecting DNA breakpoints, initial experiments were conducted using synthetic DNA strands. A 99 bp double-stranded DNA (dsDNA) molecule (ESI, Table S1†) was used to validate the sensor's ability to detect single-stranded breakpoint sites. The Nt.AlwI nicking enzyme[26] was used to recognize and cleave the GGATCNNNNN sequence on the DNA strand, generating single-stranded DNA breakpoints (SSBs) without fully cleaving the DNA. The sensor was then applied to quantify DNA breakpoints before and after enzymatic treatment. As shown in Fig. 3A and B, the number of DNA breakpoints increased markedly following enzymatic cleavage.

To further validate the sensor's detection capability in biological samples, its performance was evaluated on large-fragment genomic DNA. λ DNA (31.5×10^6 Da; 48 502 bp) was selected for this study. The λ DNA was treated with the SnaB I enzyme, which recognizes the TAC/GTA sequence in λ DNA and cleaves both strands to generate blunt-ended double-stranded breaks (DSBs). Changes in DNA breakpoints were subsequently detected. As shown in Fig. 3C and D, a substantial increase in DNA breakpoints was observed following enzymatic cleavage. After detecting genomic DNA breakpoints, the sensor was applied to detect sperm DNA breakpoints. As

This journal is © The Royal Society of Chemistry 2025

Published on 20 February 2025. Downloaded by Shanghai Normal University on 2/26/2025 3:10:55 AM.

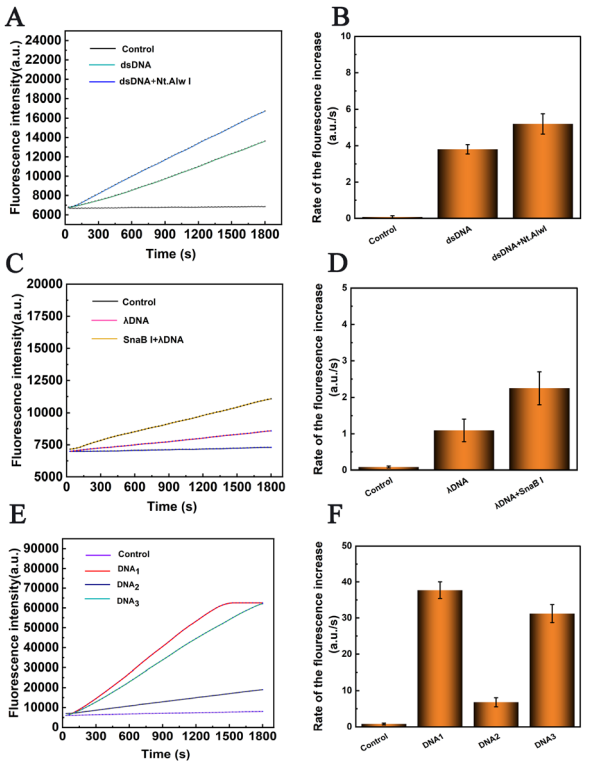


Fig. 3 Feasibility verification of the sensor for DNA breakpoint detection. (A and B) Fluorescence curves and corresponding signal increase rates for detecting DNA breakpoints in 99 bp DNA pre- and post-Nt.AlwI treatment. (C and D) Fluorescence curves and corresponding signal increase rates for detecting DNA breakpoints in λ DNA (48 502 bp) pre- and post-SnaB I treatment. (E and F) Fluorescence curves and corresponding signal increase rates for detecting DNA breakpoints in sperm DNA samples obtained from 3 patients.

shown in Fig. 3E and F, sperm DNA from three patients exhibited distinct fluorescence curves with varying slopes, reflecting variations in the number of DNA breakpoints. Using the slopes corresponding to the three indicators, Y (37.69; 6.80; 31.22), and substituting them into the standard curve equation ($Y = 265.91x + 0.5158$), the corresponding values of x (0.14; 0.024; 0.115) were obtained. Then, by substituting X (C_0) into the calculation formula (see ESI, section 1.43†), the mean number of DNA breakpoints in the sperm samples was determined:

$$\mathrm{MDB}_1 = 1.363 \times 10^5,\ \mathrm{MDB}_2 = 0.230 \times 10^5,$$
$$\text{and}\ \mathrm{MDB}_3 = 1.126 \times 10^5.$$

To establish a standard curve, synthetic short single-stranded DNA (ssDNA) was used. However, significant molecular differences between the target analyte (sperm genomic DNA, a long and complex biomacromolecule) and the calibration standard (synthetic ssDNA) may lead to discrepancies in breakpoint quantification (MDB) calibration. To evaluate the system's accuracy, spike-and-recovery experiments were performed to assess the impact of random errors (*e.g.*, operational or instrumental errors) and systematic errors (*e.g.*, matrix effects or non-equivalence).[22] Ten sperm DNA samples were analyzed in this experiment. The initial breakpoint values (MDB_1) were recorded, followed by the addition of 0.1 nM synthetic ssDNA to each sample. After spiking, the breakpoint values (MDB_2) were measured.

$$\text{Recovery Rate}\ (\%) = [(\mathrm{MDB}_2 - \mathrm{MDB}_1)\ \div\ 0.1\ \mathrm{nM}] \times 100\%$$

As shown in the ESI (Table S2†), recovery rates for the 10 samples ranged from 85.96% to 107.12%, with an average recovery rate of 98.0% ± 8.2%. These results confirm the accuracy and reliability of the sensor system in detecting DNA breakpoints. Additionally, the stability and reproducibility of this biosensing technology were evaluated. As shown in (ESI, Table S3†), the intraday relative standard deviation (RSD) for the same sperm DNA ranged from 1.93% to 4.99%, whereas the interday relative standard deviation (RSD) was 3.48%.

Ten sperm samples were randomly selected, and their genomic DNA was extracted and MDB values measured. The extracted DNA underwent a second round of extraction, and MDB values were measured again. As shown in (ESI, Fig. S2†), the MDB values after two rounds of extraction were similar to those after one round, with no statistically significant difference. These results confirm that the extraction process does not introduce artificial breakpoints into sperm genomic DNA.

To assess the biosensor's effectiveness in practical applications, oxidative damage to sperm DNA caused by reactive oxygen species (ROS) was first examined, using hydrogen peroxide to simulate the damage. The impact of different exposure durations (15, 30, 45, and 60 minutes) on the number of sperm DNA breakpoints was analyzed. The results showed a significant increase in DNA breakage after 60 minutes of exposure, approximately four times the baseline level (Fig. 4A). This experiment highlights the biosensor's ability to assess oxidative stress-induced damage to sperm DNA. Additionally, the biosensor's clinical potential in disease diagnosis was validated by analyzing sperm samples from different populations. First, sperm samples with normal semen parameters were compared to those from patients with asthenozoospermia. The results (Fig. 4B) showed that the number of DNA breakpoints in asthenozoospermia samples (8.01×10^5) was significantly higher than in normal samples (4.78×10^5). This indicates that the biosensor can effectively distinguish between samples with varying semen quality. Furthermore, we analyzed sperm samples from patients with idiopathic recurrent pregnancy loss (RPL) and healthy individuals. The results (Fig. 4C) revealed that the number of DNA breakpoints in RPL patients (11.86×10^5) was markedly higher than in healthy individuals (4.96×10^5). This suggest that the biosensor can not only evaluate semen quality but also provide valuable insights for diagnosing specific conditions, such as idiopathic recurrent pregnancy loss. In conclusion, the biosensor demonstrates significant clinical value in assessing sperm DNA damage caused by external factors and detecting disease-associated sperm DNA damage. It provides effective support for evaluating male fertility and diagnosing related conditions. The applicability of the biosensor in detecting

Published on 20 February 2025. Downloaded by Shanghai Normal University on 2/26/2025 3:10:55 AM.

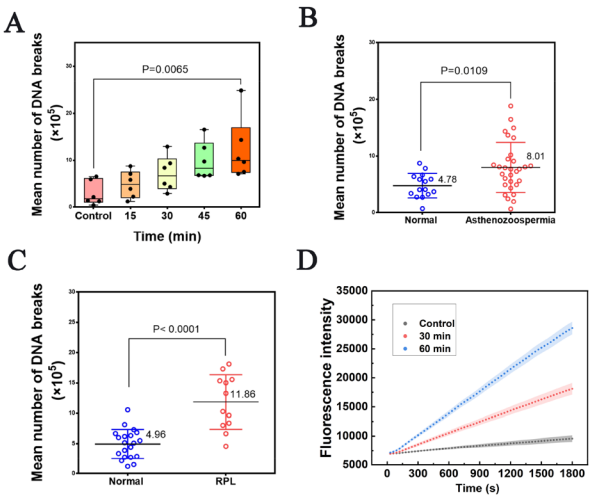


Fig. 4 The applications of the biosensor in various scenarios: (A) sperm DNA breakpoints under different hydrogen peroxide exposure durations (15, 30, 45, and 60 minutes, n = 6). (B) Detection of sperm DNA breakpoints in normal individuals (n = 15) and asthenozoospermia patients (n = 30). (C) Detection of sperm DNA breakpoints in patients with idiopathic recurrent pregnancy loss (RPL, n = 12) and healthy individuals (normal, n = 20). (D) Detection of spermatogonial stem cell DNA damage under heat stress conditions (n = 3).

DNA breakage in other reproductive cells was further explored. Spermatogonial stem cells were used as a model to assess DNA damage under heat stress conditions. The results (Fig. 4D) indicated a significant increase in DNA breakpoints in spermatogonial stem cells under heat stress, which further escalated with prolonged stress exposure. These findings suggest that the biosensor is not only suitable for assessing sperm DNA damage but also broadly applicable for monitoring the health of other reproductive cells, studying environmental stress effects, and investigating the mechanisms of male infertility. This offers a novel tool and perspective for evaluating reproductive health and implementing interventions.

The primary limitation of the biosensor system lies in the time-intensive DNA extraction process, which could potentially be resolved through automated instruments following further validation. Additionally, the limited sample size highlights the need for large-scale, multicenter studies to generate comprehensive data and explore the correlation between MDB values and clinical fertility outcomes, thereby enhancing clinical applicability.

In summary, the novel biosensor, characterized by its high sensitivity and precision, demonstrates substantial potential in evaluating external stimuli, assessing male fertility, and diagnosing related conditions. By employing TdT enzyme to recognize and extend DNA breakpoints in combination with Cas12a, the biosensor achieves an exceptional breakpoint detection sensitivity of 0.99 pM. The biosensor operates without the need for expensive instruments and allows precise detection of DNA breakpoints using a fluorescence detection device. With further optimization of operational procedures and the expansion of clinical studies, this system is anticipated to become an essential diagnostic tool in male reproductive health, offering scientific support for personalized treatments and clinical decision-making.

Author contributions

Juan Wang: methodology, formal analysis, investigation, writing original draft. Fan Zhang: formal analysis, resources and writing-original draft. Ziyang Liu: investigation, data curation. Yue Zhou: data curation. Liguo Pei: resources and writing-review and editing. Bei Yan: writing-review and editing, supervision, and project administration.

Data availability

The data supporting this article have been included as part of the ESI.†

Conflicts of interest

There are no conflicts to declare.

Acknowledgements

This work was supported by the National Natural Science Foundation of China (82260290, 82460295), Ningxia Medical University Scientific Research Project (XZ2024013), Ningxia Natural Science Foundation (2024AAC03805), the China Postdoctoral Science Foundation General Foundation (2023MD744222).

References

1 T. Marić, I. Wójcik, A. Katušić Bojanac, A. Matijević, M. Ceppi, M. Bruzzone, E. Evgeni, T. Petrović, I. Trbojević-Akmačić, G. Lauc, D. Ježek and A. Fučić, *Reprod. Toxicol.*, 2022, **113**, 96–102.
2 M. Hosseini, A. Khalafiyan, M. Zare, H. Karimzadeh, B. Bahrami, B. Hammami and M. Kazemi, *Hum. Genomics*, 2024, **18**, 57.
3 R. Musson, Ł. Gąsior, S. Bisogno and G. E. Ptak, *Hum. Reprod. Update*, 2022, **28**, 376–399.
4 A. Agarwal, M. K. Panner Selvam, S. Baskaran and C. L. Cho, *Expert Rev. Mol. Diagn.*, 2019, **19**, 443–457.
5 W. Yuan, G. Ji, X. Shi, Z. Sun, C. Liu, Y. Yu, W. Li, X. Wang and H. Hu, *Ecotoxicol. Environ. Saf.*, 2024, **278**, 116465.
6 A. García-Rodríguez, J. Gosálvez, A. Agarwal, R. Roy and S. Johnston, *Int. J. Mol. Sci.*, 2019, **20**, 31.
7 G. Talibova, Y. Bilmez and S. Ozturk, *DNA Repair*, 2022, **118**, 103386.
8 C. Ritchie and E. Y. Ko, *Andrologia*, 2021, **53**, e13581.
9 F. Li, X. Duan, M. Li and X. Ma, *Sci. Rep.*, 2024, **14**, 356.

 This journal is © The Royal Society of Chemistry 2025

Published on 20 February 2025. Downloaded by Shanghai Normal University on 2/26/2025 3:10:55 AM.

10 Y. Jiang, Z. Shen, J. Xu, J. Zhu, H. Wang, W. Chen, Y. Sun and Q. Yang, *Front. Endocrinol.*, 2023, **14**, 1168010.
11 K. Liu, X. Mao, Y. Chen and R. An, *Sci. Rep.*, 2023, **13**, 2717.
12 W. Jiang, L. Zhu, L. Gao, J. Wang, J. Fang, L. Chen and S. Wang, *Syst. Biol. Reprod. Med.*, 2024, **70**, 218–227.
13 M. Wang, J. Sun, L. Wang, X. Gao, X. Lu, Z. Wu, Y. Wang and K. Liu, *J. Assist. Reprod. Genet.*, 2014, **31**, 1655–1663.
14 I. Hervas, J. C. Martinez-Soto, M. Mollá, J. Landeras, M. Nicolás, L. Fernandez-Olmedilla, M. Trabalón, R. Rivera-Egea, M. Gil Julia and N. Garrido, *Hum. Reprod.*, 2024, **39**(1), DOI: **10.1093/humrep/deae108.391**.
15 E. Jerre, M. Bungum, D. Evenson and A. Giwercman, *Fertil. Steril.*, 2019, **112**, 46–53.
16 R. Blachman-Braun, J. C. Best, V. Sandoval, S. D. Lokeshwar, P. Patel, T. Kohn, M. Jacobs and R. Ramasamy, *F&S Rep.*, 2020, **1**, 233–238.
17 D. P. Evenson, *Anim. Reprod. Sci.*, 2016, **169**, 56–75.
18 R. Sharma, C. Iovine, A. Agarwal and R. Henkel, *Andrologia*, 2021, **53**, e13738.
19 S. Gupta, R. Sharma and A. Agarwal, *Curr. Protoc. Toxicol.*, 2017, **74**, 16.11.11–16.11.22.
20 R. Sharma, S. Forte, S. Gupta, Z. Cakar, C. DeGeyter and A. Agarwal, *Fertil. Steril.*, 2016, **106**(3), e288–e289.
21 B. Yan, W. Ye, J. Wang, S. Jia, X. Gu, H. Hu, W. Xiang, T. Wu and X. Xiao, *Clin. Chem.*, 2022, **68**, 540–549.
22 B. Yan, H. Fan, H. Ji, S. Li, H. Hu, X. Gu, S. Jia, Y. Liu, J. Guo, Z. Yang, L. Zhou, X. Xiao, L. Li and Z. Mao, *Anal. Chim. Acta*, 2023, **1280**, 341821.
23 L. T. Nguyen, B. M. Smith and P. K. Jain, *Nat. Commun.*, 2020, **11**, 4906.
24 G. Tian, D. Zhang, Y. Wang, T. Hu, Y. Lin, Y. Wang, W. Cheng and Q. Xia, *Anal. Chim. Acta*, 2021, **1176**, 338755.
25 J. T. Zwerus, N. F. Berghuis, J. M. Jacques, R. Mars-Groenendijk, R. W. Busker, A. Paauw, A. L. de Jong and H. C. van Leeuwen, *Biosens. Bioelectron.*, 2024, **261**, 116464.
26 Q. Wen, D. Li, G. Huang, H. Xi, H. Pan, L. Zhang, Z. Li, X. Xiao and W. Zhu, *Analyst*, 2022, **147**, 4980–4985.